Energy Conversion and Management: X 28 (2025) 101233

Contents lists available at ScienceDirect

Energy Conversion and Management: X

journal homepage: www.sciencedirect.com/journal/energy-conversion-and-management-x

Flexibility assessment in continuous manufacturing processes based on a physics-informed digitalisation strategy: A case study in the rubber industry☆

María Herrando [a,*], Ismael Viejo [a], Susana Calvo [a], Leticia A. Gracia [a], Salvador Izquierdo [b]

[a] Instituto Tecnológico de Aragón (ITA), Zaragoza, Spain
[b] Instituto de Investigación en Ingeniería de Aragón (I3A), University of Zaragoza, Zaragoza, Spain

ARTICLE INFO

Keywords:
Co-extrusion process
Energy efficiency
Energy flexibility
Physics-informed digitalization
Product quality tolerance

ABSTRACT

This study develops a physics-informed digitalisation strategy to assess potential flexibility from different perspectives in continuous manufacturing processes. As a case study, the co-extrusion process of sealing profiles for the automotive industry is chosen. This process operates continuously for 3–5 days to manufacture one sealing profile, consuming considerable energy, which is influenced by the process conditions set during the manufacturing line start-up. Increasing flexibility can contribute to a more sustainable and energy-efficient manufacturing industry. However, since process conditions directly affect the final quality and properties of the manufactured profile, any modifications must be preceded by a thorough analysis of their implications based on the sealing profile geometry, different line velocities and product quality tolerances. Computational Fluid Dynamics (CFD) techniques are used to model the co-extrusion process, while Finite Element Methods (FEM) are applied to model product quality and temperature dependencies. A Reduced Order Model (ROM) is developed for both FEM and CFD models, and the developed model enables the assessment of optimal process parameter adjustments to accommodate line velocity changes at different product quality tolerances. The results prove that the variation of the line velocity can provide process flexibility to the industry (around ± 30 % in total electrical power for ± 20 % variation in the line velocity). Besides, a 20 % increase in line velocity results in a 5.5 % reduction in total CO_2 emissions and a 5.2 % decrease in energy costs, suggesting that operating at higher line velocities is more energy efficient. The proposed strategy also analyses the potential flexibility depending on the product quality tolerance and the utility prices. The results show that increasing the allowable quality tolerance reduces the overall power consumption, with the largest potential in thermal power reduction. Beyond the analysis of one manufacturing line in operation, flexibility can be achieved by adequately scheduling several profiles with different electrical-to-thermal power ratios. In addition, a convenient redesign of profiles can also be used, as profiles with thinner walls and less rubber allow more flexibility, although they consume more electricity in the extruder.

1. Introduction

The increase in the share of renewable energy is essential to achieving climate neutrality by 2050, as stated in the EU Green Deal [1]. This transition leads to larger fluctuations in electricity generation and pricing, potentially posing risks to the security of supply in the electric grid. This issue can only be addressed by simultaneously acting on both the supply and demand sides. Focusing solely on the supply side – for example, by shutting down power plants or activating traditional reserves – could lead to social costs and hinder the achievement of the Green Deal's primary objective.

The global industrial sector consumes more than half of the total delivered energy, and it is expected to remain the largest energy consumer of energy through 2040 [2]. As a result, it can play a crucial role in achieving energy transition goals, such as mitigating fluctuations in renewable energy generation and balancing demand and supply [3]. The conventional demand response approach in the industry – reducing load during peak hours – is no longer sufficient to achieve the required flexibility due to the growing share of variable renewable electricity in

☆ This article is part of a special issue entitled: 'SDEWES 2024_ECMX' published in Energy Conversion and Management: X.

* Corresponding author.
E-mail address: mherrando@ita.es (M. Herrando).

https://doi.org/10.1016/j.ecmx.2025.101233
Received 9 April 2025; Received in revised form 3 July 2025; Accepted 26 August 2025
Available online 1 September 2025

Nomenclature

Acronyms/abbreviations

ACC	Model accuracy
CCD	Central Composite Design
CFD	Computational Fluid Dynamics
CPD	Canonical Polyadic Decomposition
DoE	Design of Experiments
EPDM	Ethylene Propylene Diene Monomer
FE	Finite Element
FEM	Finite Element Method
IR	Infrared
LHS	Latin Hypercube Sampling
MAPE	Mean Absolute Percentage Error
MW	Microwave
ROM	Reduced Order Model
GC	Gas Convection

Symbols

α	vulcanization degree
β	foaming degree
c_e	electricity price (€/kWh)
c_{ng}	natural gas price (€/kWh)
E_e	electricity consumption (kWh)
E_{th}	thermal energy consumption (kWh)
f_e	CO_2 emission factor of electricity (kg CO_2/kWh)
f_{ng}	CO_2 emission factor of natural gas (kg CO_2/kWh)
P_e	electrical power (kW)
P_{th}	thermal power (kW)
Q	product quality

the grid [4]. Larger flexibility in the production processes, alongside on-site energy supply and storage technologies, must be implemented [5]. Industries can enhance energy flexibility by adjusting specific energy-intensive processes without compromising product manufacturing, allowing production to external factors [4]. This flexibility enables industries to shift electricity demand to periods of higher availability or lower overall demand [6]. Recent research [7] reveals that energy flexibility can significantly reduce total annual costs, operational carbon footprint, and decarbonization expenses (by 19–80 %, depending on electricity and carbon emission factors) while also decreasing reliance on fossil energy.

Nevertheless, achieving flexibility in continuous manufacturing processes remains a complex challenge for industries. Production operates in an uncertain environment with various constraints and interdependencies that must be identified and managed. Additionally, factors such as product quality, delivery schedules, and machine operating parameters must be considered. External and internal disturbances can also disrupt planned production processes, requiring companies to react effectively to stay competitive and ensure defect-free products. Flexibility enhancement in manufacturing systems not only improves efficiency but also strengthens market resilience [5]. In this context, the digitalization of manufacturing processes is gaining increasing attention, as it is believed to be a transformative force with the potential to reshape societal, economic, and environmental processes on a global scale [8]. As a result, decision support tools become essential to assist industries in making strategic and operational decisions [9,10].

1.1. State of the Art

To meet the growing demands of sustainable production [11] and ensure economic competitiveness [12], the automotive industry must lower the energy intensity of its manufacturing processes and reduce CO_2 emissions [13]. To achieve these goals, industrial systems are increasingly evolving into cyber-physical systems [14,15]. This study focuses on developing a physics-informed digitalisation strategy aimed at enhancing the energy efficiency and flexibility of continuous manufacturing processes, such as the sealing system production in the automotive industry, with a particular focus on the co-extrusion of EPDM rubber. This process is notable for its significant consumption of both electrical and thermal energy, requiring improvements in energy efficiency. Moreover, energy flexibility in continuous manufacturing is impeded by inherently long characteristic times, resulting in a slow response to changes. Therefore, understanding and analysing energy consumption at every stage of the production process becomes crucial for optimizing manufacturing processes, increasing energy efficiency [16] and enabling energy flexibility alternatives [17]. Previous research [16] proves that implementing energy-efficiency measures and adopting smart energy management technology can reduce energy consumption by up to 50 % compared to operational improvements alone, which typically achieve a 10–20 % reduction.

Continuous processes must evolve to align with the current environmental and geopolitical energy landscape, necessitating further improvements in energy efficiency to reduce CO_2 emissions [10]. Additionally, enhancing energy flexibility is crucial to compensate for the variability in renewable energy production and to adjust to fluctuating prices and availability of fossil fuels [4,18]. Consequently, flexibility is becoming increasingly vital for manufacturing systems [3], yet its implementation in continuous processes, particularly those reliant on fossil fuels [7] remains a significant challenge. Addressing this need for flexibility, integrating numerical tools into process digital twins has been suggested as a beneficial strategy [16]. A robust numerical approach must tackle several key aspects, including developing accurate physics-based or physics-informed models for process design; creating real-time or process-time predictive models for optimal control; constructing multiscale and multi-agent models that integrate separate models for machinery, processes, and buildings; and applying multi-objective optimization algorithms for balancing energy, cost and quality requirements [19]. This work applies multi-objective optimization algorithms to physics-informed models to assess energy, cost and quality requirements.

Continuous manufacturing processes considered in this discussion are those where materials are continuously fed into the system, and products are continuously produced without interruption. These products can be a bulk material, or fluid, or a continuous product (continuous production of discrete products is not considered). Examples include chemical processes like those in biorefineries [20], pharmaceutical manufacturing [21], food and beverage production [22], or paper and pulp manufacturing [23]. Traditionally, energy management in continuous processes involves prioritising the following [24]: implementing real-time monitoring systems, utilizing advanced automation and control technologies, integrating energy-efficient manufacturing paradigms such as lean manufacturing, adopting strategic policies and frameworks that align with industry standards, leveraging information and communication technologies (ICT), regularly assessing and upgrading equipment, and training employees on energy-conscious behaviours.

Among the different types of digital tools that can be developed [25], data-driven approaches have gained increasing attention [26]. However, while developing physics-based models is more resource-intensive, they offer significant advantages. They can generate large and noise-free datasets for any combination of input parameters [27,28] and are not constrained by output limitations, as seen in data-driven models. Additionally, physics-based models provide a deeper understanding of the process, enabling virtual simulation under varying conditions. The

physics-informed digitalization strategy proposed in this research integrates physics-based models of industrial processes with real data from the manufacturing process, enhancing accuracy and applicability.

1.2. The case study

Automotive sealing profiles are installed in vehicles to ensure water and sound insulation between different parts of the vehicle body. They are typically made of EPDM rubber or TPE, combined with metallic or glass fibre hoop reinforcements and are manufactured through co-extrusion processes. The co-extrusion process of EPDM rubber is performed along a continuous production line of about 120 m long with the following successive sub-processes (see Fig. 1): i) preforming of the metal carrier, ii) co-extrusion of EPDM rubber through a die-head, ii) simultaneously curing and foaming through several ovens (thermal treatments) using several oven technologies (infrared, microwave and gas convection ovens) to achieve the desired final properties, and iv) cooling and additional finishing steps.

In the manufacturing process, first, the different rubber components flow through the channels of the die-head, which are fed by three extruder screws. The reinforcement elements (e.g., a metal band or glass fibre hoops) are introduced in the die head at this stage, together with foaming agents, when necessary. As shown in Fig. 1, the next stage involves the curing and foaming processes, which start at the die-head exit, through an infrared (IR) oven, a microwave (MW) oven, and two gas convection (GC) ovens with a cooling bath in between. These thermal treatments activate the curing and foaming processes, so their synchronisation is critical to reaching the desired product quality. The main goal of the IR oven is to seal and cure the outer layer of the sealing profile, which exits the oven at around 120–140 °C. Afterwards, the profile enters the MW oven, which heats it from the inside and starts the foaming process. The sealing profile leaves this oven at around 140–160 °C and enters a gas convection oven to continue the curing and foaming processes simultaneously. It then passes through a cooling bath to lower its temperature before entering a second gas convection oven to complete the curing and foaming, exiting the oven around 160–190 °C.

The manufacturing parameters of these lines, particularly those associated with the curing and foaming mechanisms, have a significant impact on the final shape and properties of the sealing profile, which are key factors in meeting product quality standards. The shape of the sealing profile is critical to ensure effective water and sound isolation, meaning any manufacturing deviations that affect the shape must be avoided. Still, these parameters are often adjusted using trial-and-error methods. For this reason, manufacturers usually operate their production lines with fixed parameters [29]. Nevertheless, increasing the flexibility of these processes is a primary objective for manufacturers as it would not only enhance product quality but also contribute to sustainability goals.

The rubber extrusion process operates continuously for extended periods (3–5 days), producing the same sealing profile at a constant velocity, with associated process parameters fixed for the rest of the equipment. Fig. 2 shows the electrical power consumed to produce a sealing profile over several days, which proves its stability over time. The mean value is 91.95 kW, with most electricity consumption monitored within ± 5 % and all electricity consumption within ± 10 %. Therefore, the manufacturing process of a sealing profile has constant process parameters and can be assumed to have a constant electricity consumption throughout the process, which lasts several days. For this reason, the manufacturing company has contracts with the utilities with fixed prices during the day and fixed CO_2 emissions costs as well. The prices considered in this manuscript are their current ones, which are negotiated once per year with the utilities.

Meanwhile, the velocity can change when switching to a different sealing profile; an extensive procedure is needed to set the appropriate process parameters that ensure the required product quality. Therefore, there is currently no flexibility in energy consumption; the manufacturing lines cannot be paused for demand response or adjusted

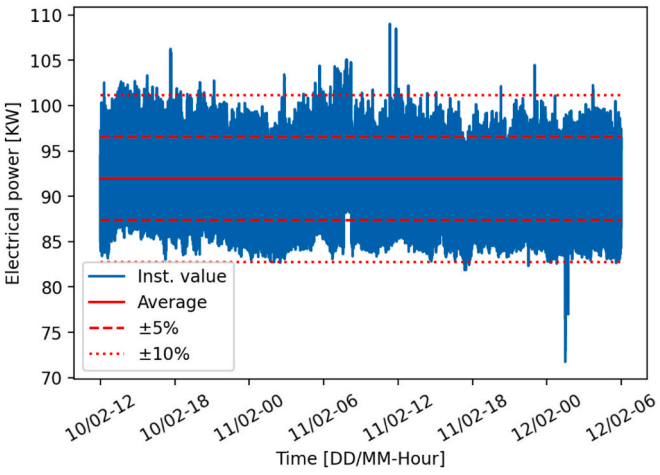

Fig. 2. Electrical power of a manufacturing line during the production of a sealing profile.

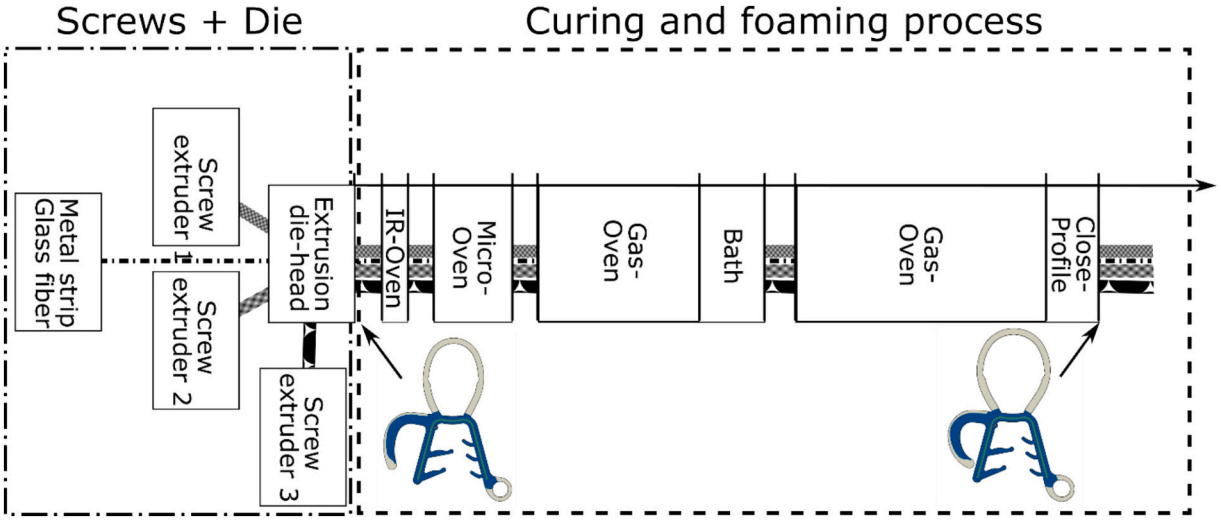

Fig. 1. The co-extrusion process.

based on electricity prices. The physics-informed digitalisation strategy proposed in this work provides real-time insights into the energy consumption of the manufacturing lines operating at different velocities, along with the required process parameter values needed to achieve the desired product quality. This approach can be used as a decision support tool, enabling greater energy flexibility within the manufacturing process.

The quality of the sealing profile is mainly based on the curing level and dimension of the profile, the online determination in real-time being the best option. In this context, certain trends in online inspection are worth noting, such as the possibility of performing a visual inspection of the profile [30]. However, this method only captures the external profile and does not allow for measurements of internal thicknesses, which are the key performance indicators (KPIs) typically measured later in the laboratory. Another possibility arises from indirect mechanical measurements through the analysis of vibration responses [31]. However, the length of the production line, its continuous operation, and the coextrusion of metallic components limit the practical application of this approach for continuous in-line measurements. It is noteworthy that the development of intelligent sensors incorporating AI-assisted techniques, as well as data-driven and physics-based models with limited online sensing (e.g. vision or vibration), can enable accurate control of certain quality parameters [32]. Even more promisingly, these advancements could allow for proper quantification and management of uncertainty [33].

Developing useful digital tools in continuous processes, such as the automotive sealing manufacturing process, requires establishing reliable numerical models for the physical mechanisms occurring during the manufacturing of the profile. While the simulation of the extrusion profile sections is well-documented in the literature [34–36] and even available through commercial software, modelling the curing and foaming processes of rubber remains relatively novel [37]. Separately, rubber curing (vulcanisation) and foaming mechanisms have been studied experimentally [38–40] and numerically [41–43]. The most common approach for capturing the combined effects of curing and foaming is solving the thermal-kinematic coupling using Finite Element Methods (FEM) [44]. Most recent works introduce coupling strategies based on the commercial software Abaqus [45], including kinetic fields via user-defined subroutines [46,47]. However, these studies have mainly focused on tire modelling [48], with limited research on the continuous extrusion processes. In addition, existing models predominantly emphasize material properties [46,48], overlooking or even dismissing the energy consumed during the process. As a result, there is a significant gap in the literature regarding the analysis of energy consumption and flexibility in the rubber industry.

1.3. Novelty and Objectives

Previous research [49] concluded that the deployment of integrated, user-friendly and efficient decision support tools still requires extensive research, both on the manufacturing process side to tackle different mathematical approaches and to develop more robust user-control planning tools [3]. This research aims to enhance industrial flexibility and energy efficiency by developing a physics-informed digitalization strategy for continuous manufacturing processes, addressing complex operational scenarios and critical challenges identified in previous research [19]. The co-extrusion manufacturing process in the rubber industry is presented as a case study, analysing potential flexibility from different perspectives (process, product quality, cost) to provide the manufacturer with a decision support tool for production planning and energy efficiency improvement, accounting for the flexibility of the line. The complexity of the developed numerical models involves the coupling between the kinetics, thermal, and mechanical fields required to model the key manufacturing process steps −extrusion, curing and foaming- with enough accuracy to realistically replicate the process performance [33]. A novel contribution of this work is the integration of the energy consumption of the processes into numerical physics-based models, considering both the electrical and thermal (natural gas) consumption. Additionally, a multi-objective optimization of the process parameters is implemented to minimise energy consumption while preserving product quality, enabling more effective production planning. To this end, a set of optimization analyses is performed to determine the operational parameters at varying manufacturing line velocities, ensuring that: i) product quality is maintained and ii) energy consumption is minimised, increasing the tolerance of product quality. The developed model allows the selection of the sealing profile to be manufactured, the line velocity, the utility (electricity and natural gas) prices, the CO_2 emission factors, and the quality tolerance level, and provides as outputs, among others, the total power (thermal and electrical) required by the main processes, the energy consumed to manufacture a specific amount of sealing profile (set by the user) and the associated CO_2 emissions and energy costs. Results obtained from the model are analysed considering the potential flexibility depending on the product quality tolerance and the utility prices.

2. Methodology

The physics-informed digitalisation strategy involves the development of different modelling methodologies depending on the physics of the process. Computational Fluid Dynamics (CFD) techniques are used to model the processes dominated by fluid dynamics (co-extrusion process), while an analysis using Finite Element Methods (FEM) is applied to model shape-related profile details (product quality) and temperature dependencies (curing and foaming process). Due to the high computational cost of traditional techniques, Reduced Order Models (ROMs) are developed for both FEM and CFD models, significantly decreasing computation time and enabling real-time execution of the manufacturing line model. These ROMs are used in some optimisation algorithms to provide optimal solutions (see Fig. 3).

The main inputs to the manufacturing line model are the geometry of the profile section, the line velocity and the product quality (referring to the tolerance in product quality, see Section 2.5) to assess potential flexibility. The main outputs are the power (thermal, P_{th}, and electrical, P_e) required, the energy (thermal, E_{th}, and electrical, E_e) consumed to manufacture a specific amount of sealing profile (set by the end-user), and the associated CO_2 emissions (Em_T) and energy costs (c_T) (see Fig. 3). The CO_2 emission factors, f_{ng} and f_e, and the average costs of natural gas and electricity, c_{ng} and c_e, provided by the automotive sealing industry [50] are used as default values (see Table 1), although these parameters can be customised by the end-user.

$$c_T = E_{th} \cdot c_{ng} + E_e \cdot c_e \tag{1}$$

$$Em_T = E_{th} \cdot f_{ng} + E_e \cdot f_e \tag{2}$$

In the context of this work, the concept flexibility encompasses three different meanings: i) process flexibility, defined as the sensitivity to variations in the velocity, ii) product quality flexibility, defined as the tolerance level variations of product quality, and iii) cost flexibility, defined as the change in the power ratio compared to the change of utility cost ratio, which can be modulated by varying the velocity and/or product quality tolerance, and it also depends on the utility costs, as shown in Eq. (3),

$$Flexibility = \frac{P_e/P_{th}}{c_e/c_{ng}} \tag{3}$$

Two sealing profiles of the two main types of automotive profiles are modelled (see Fig. 4). The main difference between both profiles that influences energy consumption is the material thickness (profile A is thicker). Both profiles have three distinguished sections depending on the material: rubber (blue area), rubber with foaming agent (grey area)

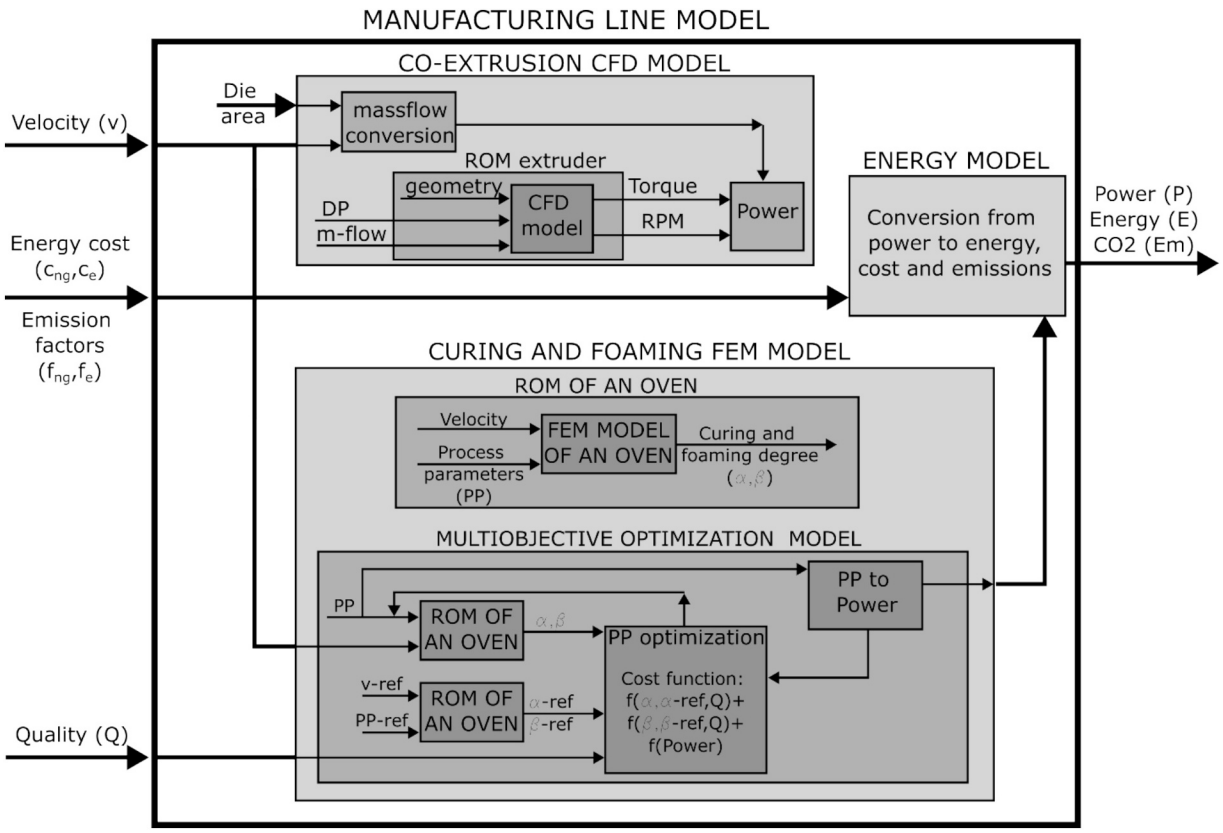

Fig. 3. Physics-informed digitalisation strategy.

Table 1
Reference values for utility prices and CO_2 emission factors.

	Utility Price (€/kWh)	CO_2 emission factor (kg CO_2/kWh)
Electricity	0.110	0.331
Natural gas	0.080	0.252

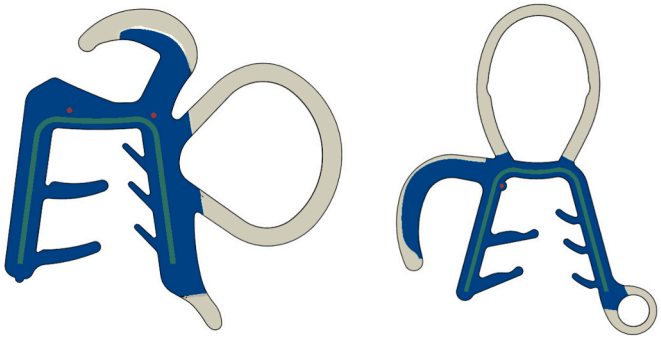

Fig. 4. Geometry of the profiles A (left) and B (right).

and metal strip (green area).

2.1. Manufacturing line model

To model the co-extrusion process of the sealing profile, two main physics-based numerical models are developed: a CFD model for the co-extrusion process within the die-head, and an FEM for the curing and foaming processes. Once these models are validated, a Design of Experiments (DoE) is defined, and the required simulations are conducted to build up a Reduced Order Model (ROM) [51,52] of each key component: extruders, IR, MW, and GC ovens. This approach involves the creation of surrogate models using a tensor factorisation technique, implemented using the TWINKLE library [51]. This library is based on Canonical Polyadic Decomposition (CPD) of tensors, preserving the physics behind the phenomena and keeping the input variables in the final output result. Additionally, the library allows the reduction of non-structured and sparse data sets, as those generated by a series of numerical experiments when applying DoE approaches. Due to this capability, the DoE strategy used is a Central Composite Design (CCD), with the limits of the domain to be explored, ensuring that the evaluation is performed without doing extrapolations; and a Latin Hypercube Sampling (LHS) to explore the inner domain. One of the main advantages of the explainability of the resultant models is that the solution can be represented (see Ref. [48] for more details of this representation), and therefore, some important aspects of these reductions, such as overfitting, can be visually detected. The main result of the ROMs is the relationship between the power required vs. line velocity of the key components (IR, MW and GC ovens). These ROMs allow for assimilating monitored data from the line and are integrated into the manufacturing line model, which serves as a decision support tool for the manufacturer to assess flexibility from different perspectives (process, product quality and cost) and schedule production accordingly.

For the extruder, the CFD model (see Section 2.2) runs at different mass flow rates (which imply different line velocities), maintaining a constant pressure drop. The results of this DoE are used to build up a ROM of the extruder, which includes the screw torque and the screw speed at different line velocities.

For the curing and foaming process, the FEM results (see Section 2.3) are used to develop a ROM that relates the resulting profile conditions (i.e. contours of temperature and curing and foaming degrees within the sealing profile) that set the product quality with the input parameters (lamps' power/microwave power/gas consumption, and line velocity). This ROM is used to perform a multi-objective optimization analysis

with inputs, the line velocity and the product quality, and output, the power consumption. This multi-objective analysis requires a specific methodology as described in Section 2.5.

The electricity consumed by the CG ovens (e.g., for the air fans and motors) and the electricity consumption of other manufacturing line components (e.g., cutting machine, drill press) are taken from the real monitored data of the manufacturing line provided by the manufacturer.

2.2. Co-extrusion CFD model

A CFD model of the extruder is developed in ANSYS-Fluent, considering the 3D geometry of the extruder screw (e.g., barrel diameter, screw pitch, channel depth, flight width) [53] and the main operating parameters, outlet pressure and screw speed (rpm). It provides as global outputs, the mass flow rate (and associated linear velocity) and the screw torque, with which the power consumed by the extruder is estimated. Additionally, this model allows for analysing the distribution of shear stresses, velocity, pressures, and other parameters throughout the length of the screw (see Fig. 5).

2.3. Curing and foaming FEM

A previously developed model based on FEM [33] is used as a starting point for the simulation of the curing and foaming process in the co-extrusion manufacturing line. This model couples the thermal, mechanical, and kinetic fields using a fully coupled thermal stress analysis combined with subroutines, which is implemented in the FE code ABAQUS. The thermal stress enables the integration of thermal and mechanical fields. Consideration of the kinematic field requires developing specific subroutines to couple the thermal field by the definition of an expansion coefficient related to the foaming grade and to account for the dependence of the material properties with the vulcanization and foaming degrees to couple with the mechanical field. In this work, the calculation of energy consumption is integrated into the model, which is key for the multi-objective optimization analyses.

The manufactured sealing profile is a 3D geometry, but its section (2D geometry) is constant along the profile length, except for the changes produced due to the ovens, so the model can be approached as a 2D simulation, assuming plane strain. However, in the foaming zone of the sealing (see grey area in Fig. 4), an initial pre-strain state is generated that compromises the use of a 2D model. To address this, a 2.5D model is defined, where the longitudinal dimension is very short and boundary conditions equivalent to a plane strain state are defined. To account for varying conditions along the length of the sealing profile, all boundary conditions are defined as time-dependent [33].

The FE model includes the IR, MW, and GC ovens. The IR oven considers the view factors pre-calculated using ANSYS-Fluent and the lamps' power. The MW oven takes into account the magnetron power, and the GC oven accounts for the temperatures of both the hot air and the sealing profile inside the oven (see Fig. 6). The models of the ovens consider the line velocity. The results of the FE model are temperature contours of the sealing profile, as well as the curing and foaming degrees at different locations of the profile section.

As described in a previous work by the authors [33], this process may involve certain uncertainties, which can be managed using the same ROM approach presented in this work. However, the focus here is on the energy consumption of complete batches of sealing profiles, which typically last 3–5 days. During this time, the manufacturing parameters generally remain constant, resulting in stable energy consumption (as shown in Fig. 2), aside from minor fluctuations caused by the machines' PID control systems and material variability. These fluctuations are typically within ± 5 % of the average value, but the average consumption remains stable, allowing this analysis to be based on averaged values.

2.4. Validation procedure

First, the results obtained from the detailed FEM and CFD models are analysed and validated with the real performance of the main components provided by the manufacturer. The CFD model provides, as a result, the mechanical power obtained from the torque and the screw speed. The mechanical power is then converted into electrical power based on the specifications of the extruder electrical motor. This electrical power calculated from the CFD results is compared with the electrical power monitored in the manufacturing line.

The curing and foaming degrees cannot be directly measured and are dependent on the temperature, so the validation of the FEM results is made by validating the temperature that can be measured at any point of the line using an IR sensor. Thus, the estimated temperature of the profile exiting each oven (IR, MW and GC) is compared with the real temperature measured by the manufacturer under real operating conditions.

The accuracy (ACC) of these models is calculated using the mean absolute percentage error (MAPE), being i the main important variables selected to obtain the accuracy, such as total energy, total power, and energy per component, as shown in Eq. (4),

$$ACC = 100\% - MAPE = 100\% - \frac{100\%}{n}\sum_{i}^{n}\left|\frac{y_{i_{measured}} - y_{i_{predicted}}}{y_{i_{measured}}}\right| \quad (4)$$

2.5. Multi-objective optimization analysis

Several chemical reactions occur during the curing and foaming process to reach the adequate curing and foaming levels to ensure good product quality. When the line velocity is changed, the process parameters should be adjusted to maintain the same product quality. Currently, at the production facilities, this variation is made manually, taking a considerable amount of time and experience. Using a physics-informed model to numerically adjust the process parameters would significantly make the operation faster and more accurate. The variation of the process parameters in an iterative way and subsequent simulation of the physics-informed (CFD/FEM) models requires a considerable amount of time for each process parameter variation. However, the physics-informed model can be compacted into a ROM that runs in real

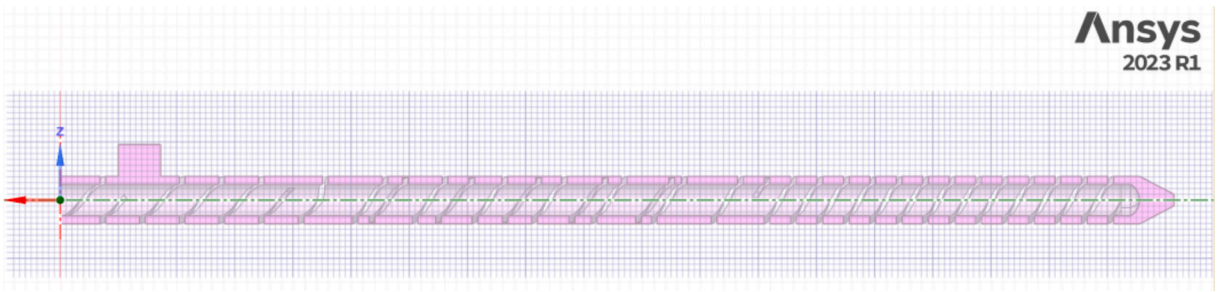

Fig. 5. CFD model of the extruder domain. Section view.

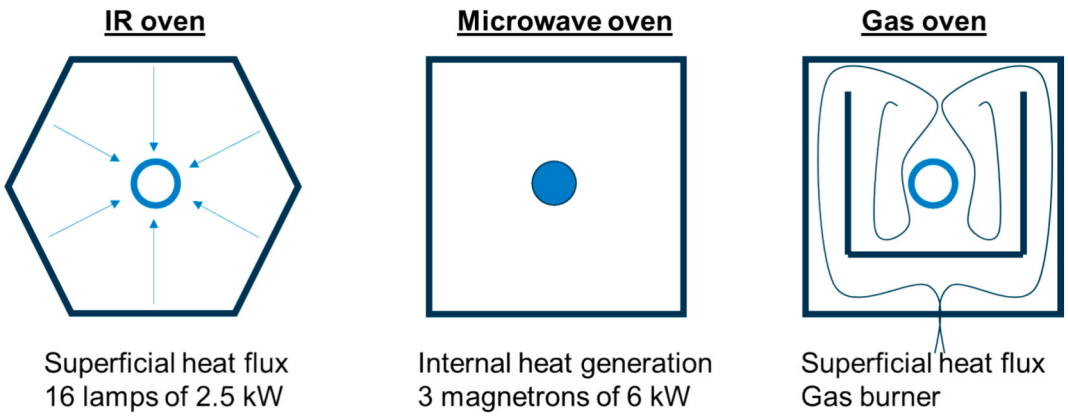

Fig. 6. Main features of the heat flux in the IR, MW, and GC ovens.

time and can be used to perform optimization analyses quickly. The multi-objective optimization analysis, summarized in Fig. 3, provides the process parameters of the oven (lamps' power, microwave power or air temperature set point in the burner) for a line velocity and a certain product quality. This analysis is performed independently for each of the four ovens: IR, MW and two GC ovens, following the same procedure for all. The only difference in the analysis concerning the ovens is the ROM used and the associated process parameters. It is important to note that each oven's performance is modelled in consideration of the preceding ovens. Specifically, during the optimization analysis of the MW oven, both the IR and MW oven models are run, while for the GC oven, the IR, MW, and GC oven models are executed. This approach is necessary because the curing and foaming processes occurring in each oven affect the subsequent one.

The optimization takes as inputs the line velocity and the product quality expressed as a percentage of error for the ROM oven's outputs (curing and foaming degrees). Additionally, a reference setup of the process parameters (including line velocity) that produces a good product quality is required. The optimization algorithm minimizes a cost function that includes multiple terms related to the energy minimization and the deviation in curing and foaming degree between the reference cases and the evaluated scenario, ensuring they remain within the specified tolerance:

$$Costfunction = \min(Power) + function(\alpha, \alpha_{ref}, Q) + function(\beta, \beta_{ref}, Q) \tag{5}$$

where, *Power* is the power consumption (thermal, P_{th}, or electrical, P_e) for the corresponding oven, α is the vulcanization degree, β is the foaming degree, and Q is the product quality (referring to the product quality tolerance).

The power minimization requires the conversion of the process parameters into power. This conversion is direct for IR and MW ovens, while the GC oven requires the change from temperature setpoint into gas consumption. This relation was obtained experimentally by the manufacturer [50]. The results considering several product quality levels are analysed in Section 3.5.

3. Results and discussion

First, the results obtained in the detailed FEM and CFD models are analysed and validated in Section 3.1 and 3.2. The CFD model of the extruder is validated by comparing the calculated electrical power with the monitored data provided by the manufacturer [50]. The FE model of the curing and foaming is validated through temperature measurements, as real-time monitoring of the curing and foaming degrees during production is not feasible. Once these physics-based models are validated, corresponding ROMs are built to generate the manufacturing line model. This model is used to assess potential flexibility from three perspectives: process flexibility (Section 3.3), product quality flexibility (Section 3.4) and cost flexibility (Section 3.5). Finally, an example of the deployment of the proposed digitalization strategy at an industrial plant [50] is presented.

3.1. Extruder results

Fig. 7 shows the pressure (left) and velocity magnitude (right) contours throughout the extruder when operating at an outlet pressure of 300 bar and a screw speed of 36 rpm, computed by the CFD model. The pressure distribution along the length of the extruder is found to be nearly linear. The velocity distribution varies depending on the geometry of each extruder section and the local position inside those sections. Additionally, the torque is computed from the fluid forces on the screw walls provided by the numerical solution. The stresses over the fluid domain calculated by the model are not shown here for space limitations, but can be used to modify and optimize the geometry and performance of the screw, or for scaling it up or down, among other applications.

To validate the extruder CFD model, the electrical power calculated is compared with the monitored extruder power provided by the manufacturer. The model accuracy (ACC) at nominal line velocity is 97.41 %. Additionally, the accuracy in predicting the power variation with velocity has been compared against data from an equivalent extruder. For this latter extruder, the CFD model provides a variation of 1.55 kW/(m/min), compared to measurement values ranging from 0.5 to 0.9 kW/(m/min). This difference arises because the CFD model assumes ideal behaviour, which did not occur in the measurement due to several factors, such as the self-heating of the rubber (lowering the viscosity) or dead recirculation zones within the extruder. The measurement would have been higher in an ideal experimental case (e.g. perfect control of temperature in the extruder).

Once the model is validated, a DoE is run to obtain a ROM that relates the screw torque and screw speed (rpm) with the mass flow rates and drop pressure (see Fig. 8 left for a specific drop pressure). The torque is then multiplied by the screw speed to calculate the mechanical power consumption of the extruder at different mass flow rates, as shown in Fig. 8 right. This ROM is an input to the overall manufacturing line model, where the drop pressure is an input that depends on the die-head drop pressure calculated using CFD simulation in the design state of the profile, and the mass flow rate depends on the line velocity and the cross-section of the profile for each material.

3.2. Curing and foaming results

The FEM of the curing and foaming mechanisms provides results for the three fields solved: i) temperatures and heat flow for the thermal

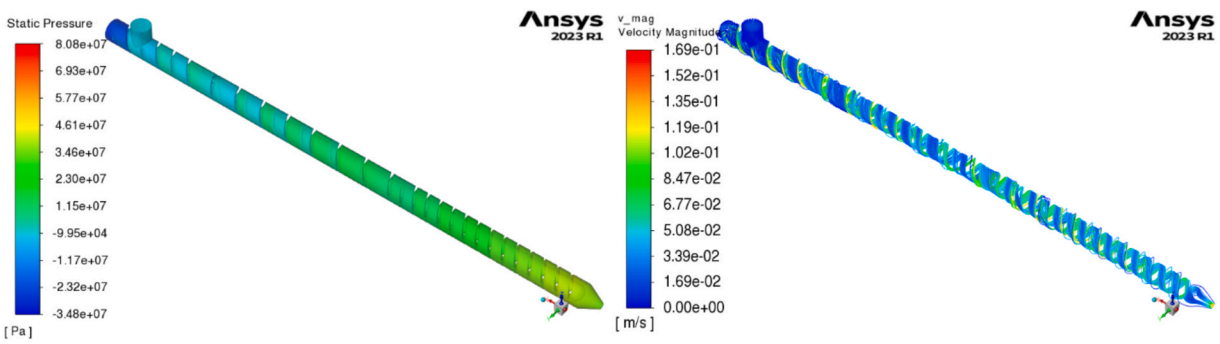

Fig. 7. Pressure contour distribution (left) and velocity magnitude path line (right) throughout the extruder.

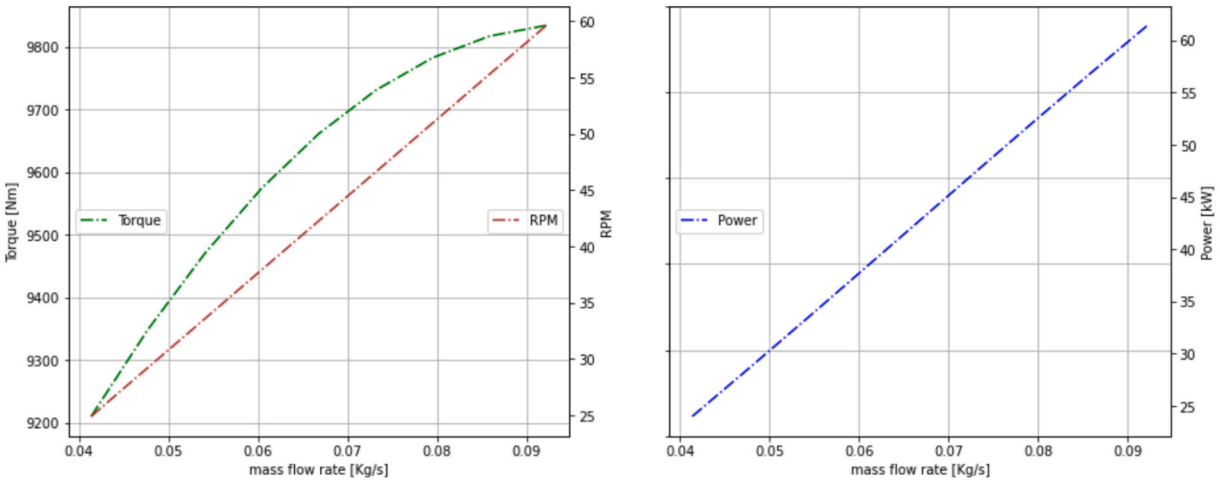

Fig. 8. Torque and screw speed (left) and mechanical power (right) of the extruder at different mass flow rates for a specific drop pressure.

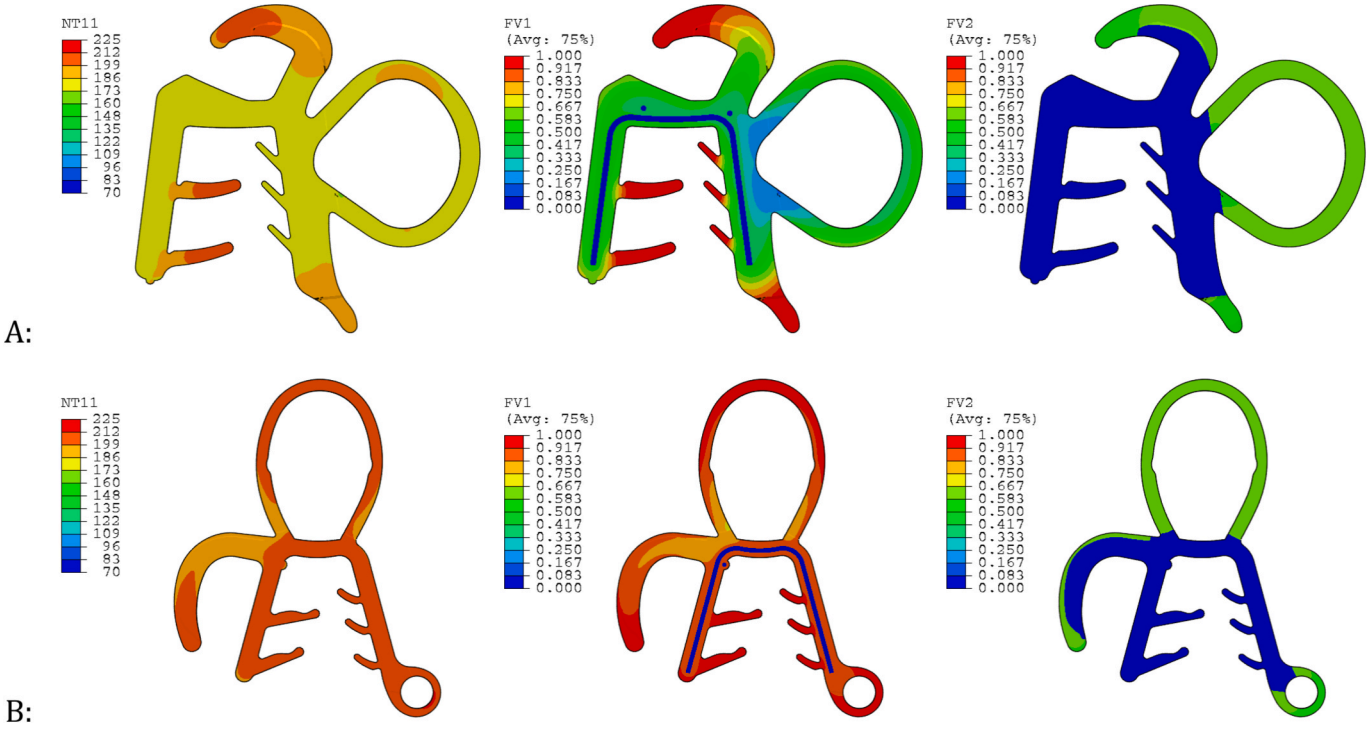

Fig. 9. Temperature contour (left), vulcanization degree contour (middle) and foaming degree contour (right) for profile A (above) and profile B (below).

field, ii) displacement and forces for the mechanical field and iii) vulcanization and foaming degrees for the kinetic field. Fig. 9 shows an example of the results of temperature, vulcanization degree and foaming degree over the deformed shape of the sealing profiles at the end of the second gas convection oven.

Fig. 10 shows the evolution of the vulcanization degree along the four thermal treatment stages of the extrusion process: i) IR oven, ii) MW oven, iii) first GC oven and iv) second GC oven. Although the vulcanization mechanisms in the profile start inside the IR oven, the achieved vulcanization level at its exit remains low and at a small area; this is the reason why it is barely noticeable in Fig. 10 left. A significant increase in vulcanization is achieved as the profile passes through the GC ovens, as noticed in the contours shown in Fig. 10 middle-right and right. Similar results are obtained for both sealing profiles. However, slight variations in the maximum vulcanization degree may occur due to differences in the selected process parameters. These parameters are adjusted through a trial-and-error approach, as real-time measurements of the vulcanization degree are highly challenging. Consequently, some variability in the peak values is expected.

The validation of the FEM is performed for the two sealing profiles. To this end, the manufacturer measured the temperature at the ovens' exit under actual operation conditions on the manufacturing line (see column "IR sensor temperature" in Table 2). These values are compared with the temperature estimated by the FEM (see column "FEM temperature").

Based on the comparison, the ACC, calculated using the nominal values (excluding the confidence interval included in Table 2), is 80.28 % for profile A and 80.24 % for profile B. As shown in Table 2, when the confidence intervals are considered, all FEM results fall within the corresponding ranges.

Further details of the validation of the vulcanisation and foaming degrees can be found in Ref. [33]. The validated FE model of the curing and foaming process is then used to build the ROM, which relates the power of the IR, MW and GC ovens with the line velocity. Similarly as for the extruder, this ROM is used to build the manufacturing line model.

Table 2
FEM validation results.

End of component	Profile A IR sensor temperature [°C]	FEM temperature [°C]	Profile B IR sensor temperature [°C]	FEM temperature [°C]
Extruder head	75 ± 10	75	108 ± 10	110
IR oven	95 ± 10	105 ± 10	135 ± 10	140 ± 15
MW oven	110 ± 10	120 ± 5	150 ± 10	132 ± 5
First GC oven	185 ± 10	170 ± 5	200 ± 10	190 ± 5
Second GC oven	190 ± 10	190 ± 5	205 ± 10	202 ± 5

3.3. Process flexibility

The manufacturing line model can be used to better understand the industrial process and analyse the sensitivity to variations of key input and process parameters. This section focuses on the influence of the line velocity, the process parameter most directly linked to process flexibility.

This analysis is performed for the two sealing profiles A and B, evaluating the required power and energy consumption per kilometre of sealing profile at different line velocities. Fig. 11 left shows that the electrical power of the extruders, IR and MW ovens and auxiliary equipment increases with the line velocity. For a ±20 % variation in the line velocity (from a nominal velocity of 16 m/min), the total electrical power varies from -30.4 % to +27.8 % in profile A (Fig. 11 above), the extruders' power from -35.3 % to +35.2 %, the IR power from -34.2 % to +36.1 %, and the MW power from -43.2 % to +16.3 %. It is observed that the thermal power of GC ovens also increases with the line velocity, but to a much lower extent (from -11.7 % to +5.2 % for a velocity variation of ±20 %). Similar results are obtained for profile B (Fig. 11 below), with the total power varying from -28.7 % to +26.2 % and the thermal power from -9.7 % to +3.1 % for a velocity variation of ±20 % from the nominal one (18 m/min). Therefore, the variation in total electrical power is primarily driven by the extruders' power, which increases linearly with the line velocity. It can also be concluded that the variation in the line velocity can potentially provide electrical flexibility to the industry while having a limited impact on the thermal power.

Fig. 12 shows the energy consumed to manufacture 1000 m of sealing profile A (above) and profile B (below). For ±20 % variation in the line velocity of profile A (from a nominal velocity of 16 m/min), the total electricity consumption varies from -13 % to +6.5 %, the extruders' consumption from -19.1 % to +12.6 %, the IR consumption from -17.7 % to +13.3 %, and the MW consumption from -29 % to -3%. Overall, there is an increase in electricity consumption, but the electricity consumed by the main components does not vary to the same extent as the increase in

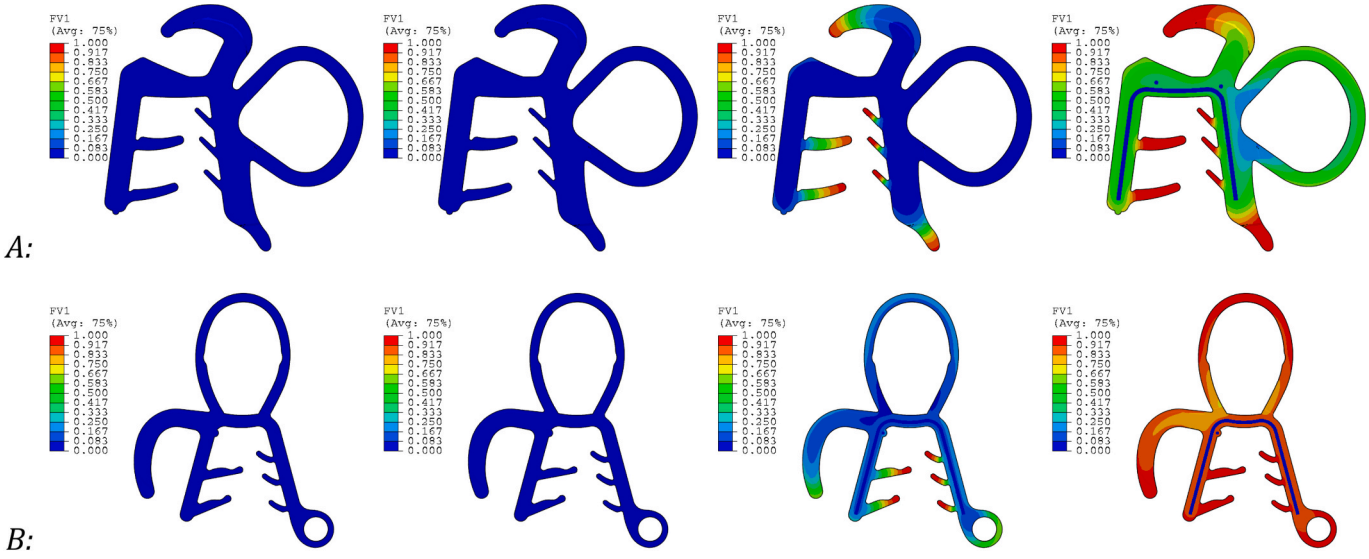

Fig. 10. Vulcanization degree distribution of the sealing profile, profile A (above) and profile B (below), over the deformed shape for the four thermal steps of the extrusion process: i) IR oven (left), ii) microwave oven (middle left), iii) first gas oven (middle right) and iv) second gas oven (right).

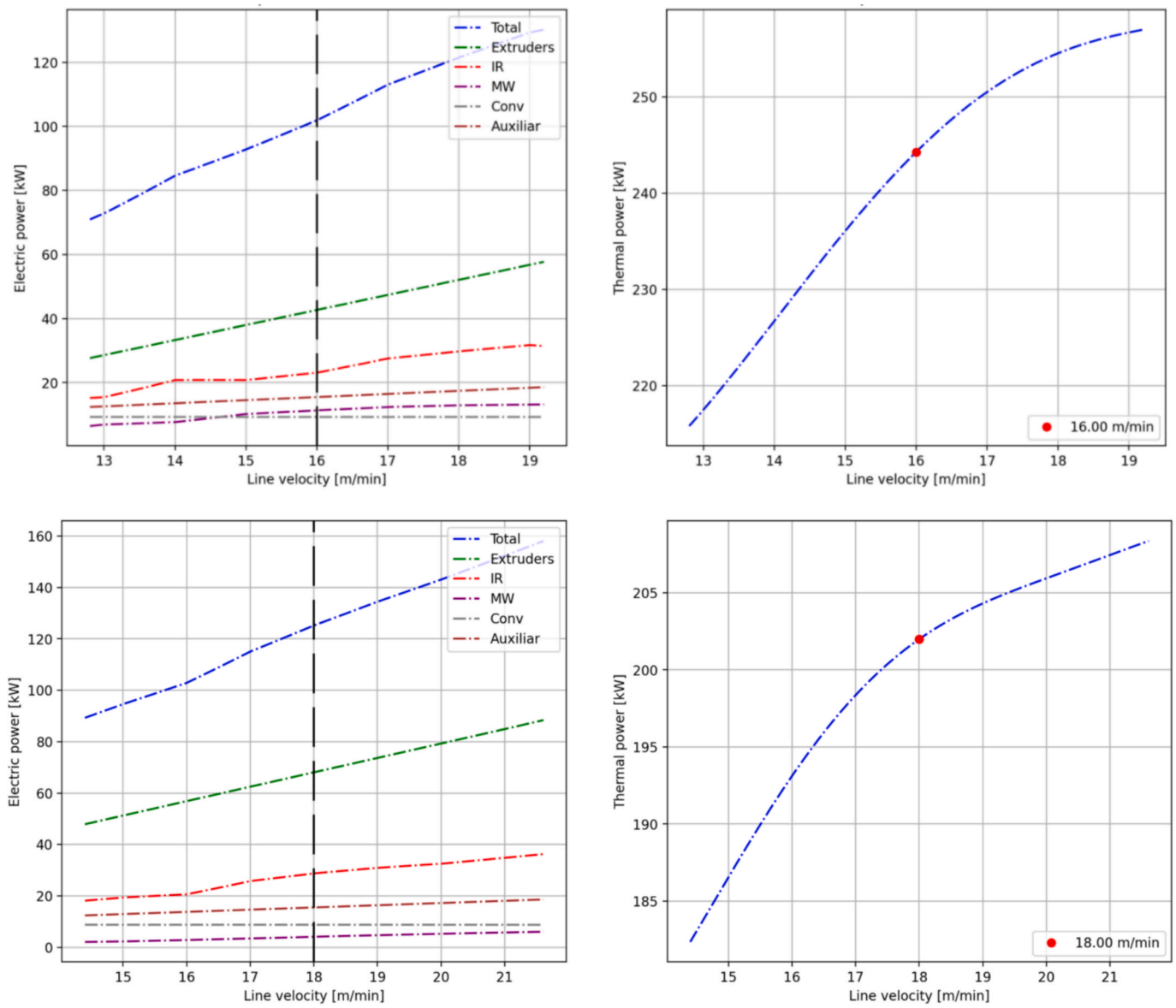

Fig. 11. Electrical (left) and thermal power (right) of the co-extrusion manufacturing line at different line velocities for profile A (above) and profile B (below).

line velocity. This is because larger velocities require higher electrical power but less manufacturing time to produce a specific amount of sealing profile. Conversely, the gas consumption decreases with the line velocity increase, with a reduction of -12.6 % when the velocity increases by 20 % compared to the nominal velocity (see Fig. 12 right). Therefore, the operation of the GC ovens at high line velocities is more efficient. Similar trends are obtained in profile B (see Fig. 12 below), with an overall increase in the electricity consumption of 5.1 % and a reduction of the gas consumption of -14.1 % for a 20 % rise in the line velocity (from a nominal velocity of 18 m/min).

It is also observed that the electricity consumed by the extruders to manufacture profile A is lower than for profile B (green line), while the gas consumed to manufacture profile A is higher than for profile B. This is attributed to the larger thickness of profile A (see Fig. 4), which leads to a lower pressure drop in the extruders but more thermal energy demand in the GC oven for the curing and foaming processes. This difference could also enable flexibility (e.g., it would be larger, as it consumes less).

The developed model also provides the results in terms of CO_2 emissions and energy costs incurred for manufacturing a specific amount of sealing profile (see Fig. 13). It is observed that the CO_2 emissions associated with gas consumption decrease with increasing line velocity (by -12.3 % for a 20 % velocity increase for profile A). In contrast, CO_2 emissions from electricity consumption rise by 7.1 % for the same velocity increase. As a result, the total CO_2 emissions show an overall reduction of -5.5 % with a 20 % increase in line velocity. Similar results are obtained in terms of energy costs (see Fig. 13 right), so high line velocities seem more efficient and a promising approach for emission and cost reduction. However, the line velocity increase is limited by the heat transfer rate inside the GC oven since a minimum residence time is required to ensure adequate curing and foaming in the profile. In this context, further work is needed to thoroughly analyse the GC oven and improve its energy efficiency at higher operating velocities.

3.4. *Product quality flexibility*

The previous analysis is extended by including product quality as an additional input parameter in the optimization algorithms to provide flexibility. This analysis yields two key outcomes: i) the industrial process parameters on product quality, and ii) the influence of product quality on production rate, energy consumption and overall process efficiency. The analysis follows the methodology outlined in Section 2.5,

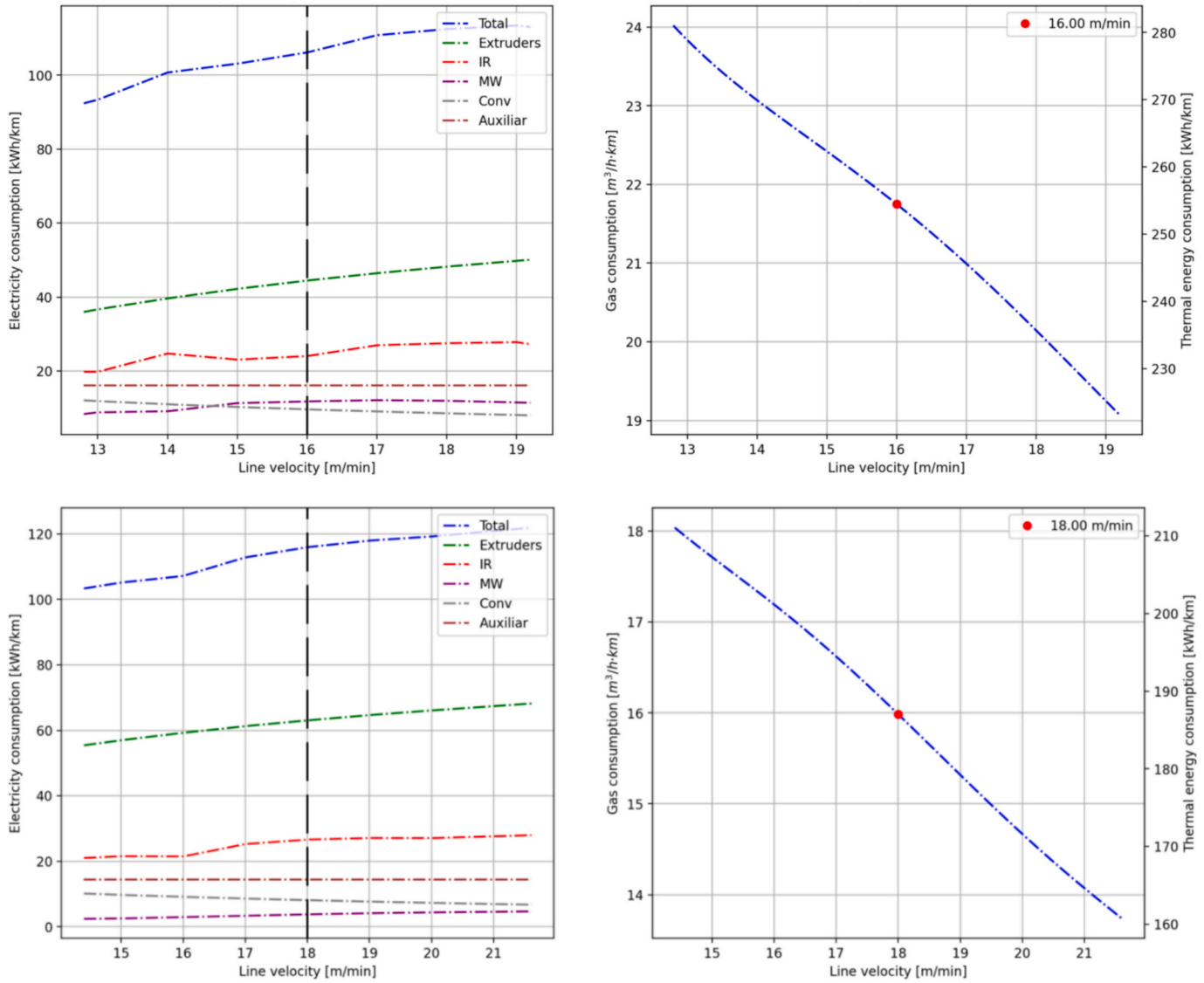

Fig. 12. Electricity (left) and thermal energy (right) consumption of the co-extrusion manufacturing line per 1000 m sealing profile manufactured at different line velocities for profile A (above) and profile B (below).

where variations in product quality tolerances are introduced in the multi-objective optimization to identify the process parameters that minimise energy consumption while quality outputs are close to the defined tolerance limits.

Three tolerances (1 %, 5 % and 10 %) are analysed, as shown in Fig. 14, which shows optimal Pareto fronts of the multi-objective analysis performed. The results show that increasing the allowable quality tolerance leads to a reduction in overall power consumption. Notably, thermal power shows the largest reduction potential (see orange line and shadow), while the electrical power used in the curing process that occurs in the IR and MW ovens (see blue line and shadow) offers comparatively less flexibility. The reason is that the curing and foaming of the profile mainly occur in the CG ovens, as shown in Section 2.2, and this process is the one that influences product quality the most. The remaining electrical power does not vary with the variation in product quality tolerance because the curing and foaming processes that set product quality do not occur in the extruders and auxiliary equipment. The power reduction with increasing quality tolerance is approximately linear. Furthermore, profile B shows a larger potential for power reduction by adjusting product quality (see Fig. 14 right), so this can also be considered for production planning depending on the utility prices. Further work is proposed to analyse the impact of increased tolerance on product quality and find the optimum tolerance level which ensures that customer requirements are met while minimizing energy consumption.

3.5. *Cost flexibility*

Finally, cost flexibility is assessed as the change in the power ratio compared to the change of the utility cost ratio. The power ratio (P_{IR+MW}/P_{th}) can be modulated by varying the velocity and/or product quality tolerance, as shown in previous sections, while the utility cost ratio (c_e/c_{ng}) is mainly imposed by the market.

Fig. 15 shows that while the cost ratio (c_e/c_{ng}) varies ±50 %, the total cost varies around ±10 %. Similar trends are found for the different product quality tolerances. Still, product quality tolerance can provide flexibility depending on the utility cost ratio. The latter is remarkable for higher quality tolerance. When considering the differences between profiles A and B, profile B provides larger flexibility as the allowed power ratio is higher, but incurring in larger total costs.

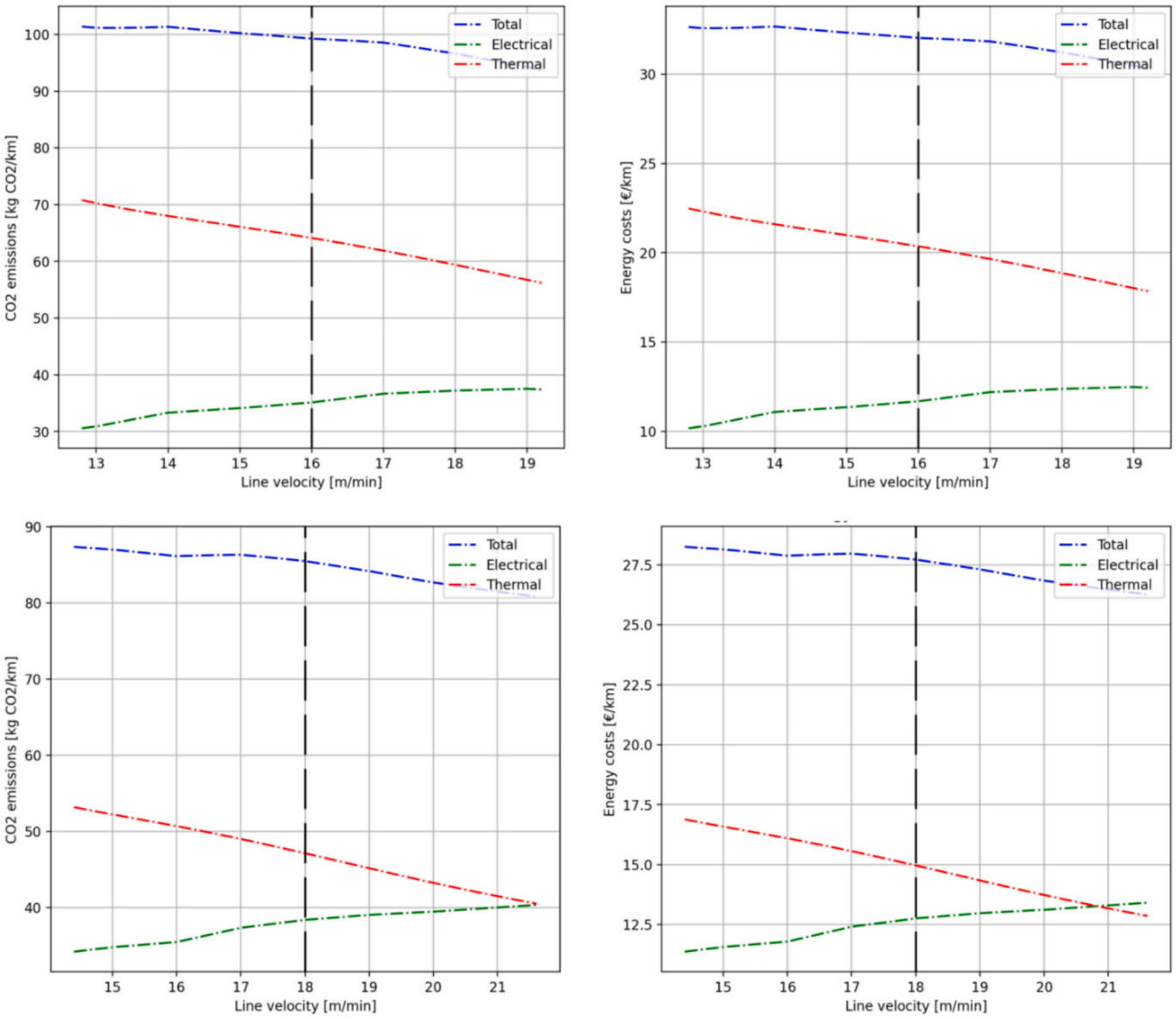

Fig. 13. CO_2 emissions (left) and energy costs (right) of the co-extrusion process per 1000 m sealing profile manufactured at different line velocities for profile A (above) and profile B (below).

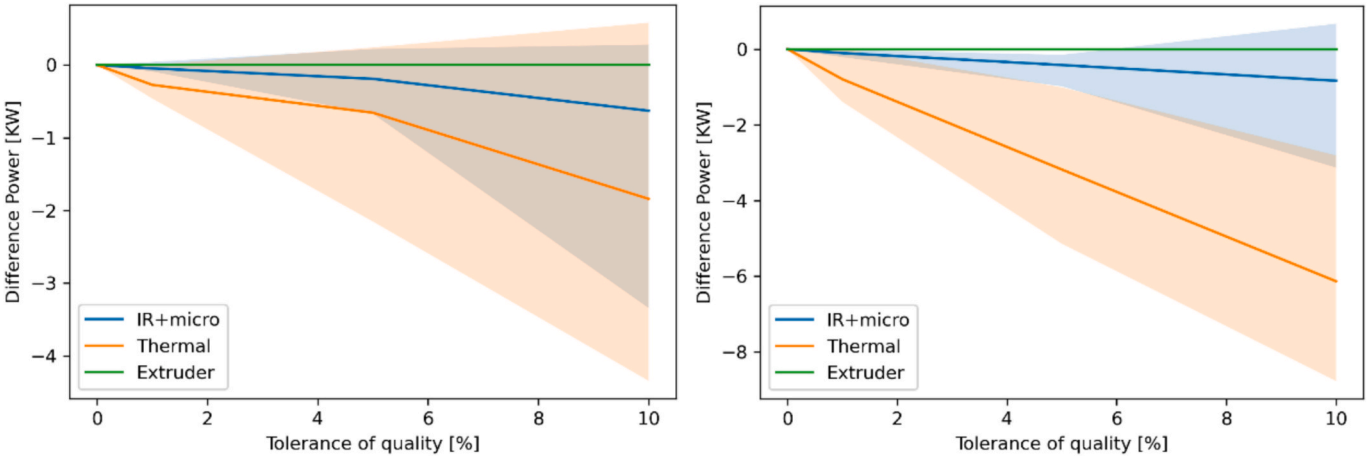

Fig. 14. Optimal Pareto fronts of the multi-objective analysis in terms of reduction in power consumption: Lines represent average values for the analysed velocity range for different tolerance levels, and shadows represent the values for the different velocities and quality tolerances for profile A (left) and profile B (right).

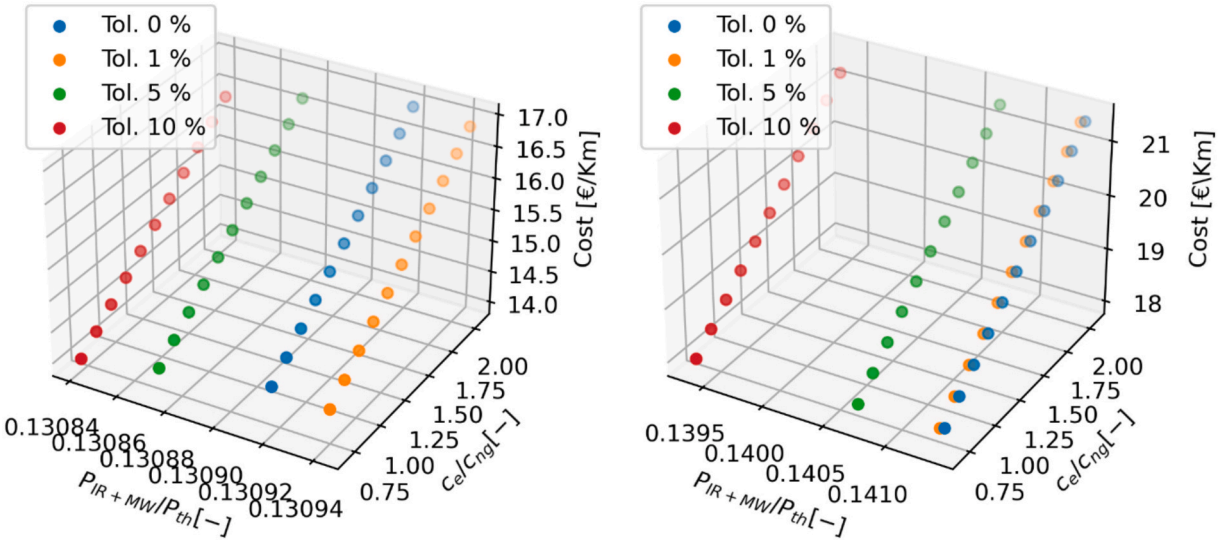

Fig. 15. Optimal Pareto fronts of the multi-objective analysis in terms of cost of manufacturing per kilometre for different power ratios and utility cost ratios evaluated for the three quality tolerances for profile A (left) and profile B (right).

3.6. Example of digitalization strategy deployment at an industrial plant

The analysis performed in this work, based on the proposed digitalization strategy, has been implemented in an industrial plant of the sealing profile manufacturer that supplied the data in the form of a web-based decision support tool (see Fig. 16).

For each of the six manufacturing lines producing rubber sealing profiles, the user can select the desired profile to be manufactured. Upon selection, the slider automatically adjusts to display the nominal velocity for that profile, and the table updates to show the total electricity consumption, the breakdown by main components (extruders, IR, MW, GC ovens and auxiliary equipment), and the total gas consumption. The user can then adjust the velocity using the slider, with energy consumption results calculated in real time. Fig. 16 illustrates in blue the energy consumption range (electricity and gas) across the velocity range, while the current energy consumption is indicated by a red line. Similar results are provided for power consumption.

4. Further discussion and conclusion

This work presents a physics-informed digitalization strategy to evaluate potential flexibility from different perspectives (process, product quality and costs) in continuous manufacturing processes. The methodology is applied to a case study involving the co-extrusion process of sealing profiles for the automotive industry.

Two main physics-based numerical models are developed to simulate the manufacturing process: a CFD model for the co-extrusion process and an FEM for the curing and foaming mechanisms. After validating these models, a DoE is defined, and the necessary simulations are run to build a ROM of the manufacturing line. Subsequently, multi-objective optimization analyses are performed to determine the process parameters for the main components of the line, considering different line velocities and product quality tolerances.

The results show that the manufacturing line offers significant potential for process flexibility. For a ±20 % variation in the line velocity (from a nominal velocity of 16 m/min in Profile A), total electrical power varies between -30.4 % and +27.8 % in Profile A, while thermal power varies more moderately, between -11.7 % and +5.2 %. This variation would allow adapting to some extent the production schedule depending on the electricity grid, for example, increasing production rates during periods of low electricity demand or low electricity prices.

The analysis also suggests that operating at higher line velocities is more energy efficient. While electricity consumption changes less significantly than the velocity variation (ranging from -13 % to +6.5 % for a ±20 % velocity variation), gas consumption decreases with increased velocity, showing a 12.6 % reduction for a 20 % velocity increase. Additionally, higher line velocities lead to reduced CO_2 emissions (-5.5 %) and energy costs (-5.2 %). This is mainly due to the lower thermal energy consumption of the GC ovens, which compensates for the increased electricity consumption from other process equipment.

Given the importance of gas consumption in the overall co-extrusion process, further work involves the development of a detailed CFD model of the GC oven to analyse in detail the heat transfer from the hot air to the sealing profile and to increase energy efficiency by minimising heat losses, which would reduce gas consumption.

The previous analysis is extended by including product quality as an additional input parameter in the optimization algorithms to provide flexibility. The results show that increasing the allowable quality tolerance reduces the overall power consumption, with the largest potential in thermal power reduction. Contingent on the tolerance level, the power reduction potential also depends on the sealing profile, so this can also be considered for flexibility potential and production planning.

Beyond assessing one manufacturing line of a specific profile in operation, flexibility can be achieved by adequately scheduling different types of profiles (thinner and thicker) with different electrical-to-thermal power ratios. In addition, a convenient redesign of profiles can also be used, as profiles with thinner walls and less rubber allow more flexibility, although they consume more electricity in the extruder.

Finally, cost flexibility is assessed as the change in the power ratio compared to the utility cost ratio variation. The results show that continuous manufacturing processes, such as the one analysed here, present narrow margins of improving the flexibility, mainly at the cost of quality tolerance (in this case); but these margins can be thoughtfully explored using fast numerical models, as the data-driven physics-informed models introduced.

In a continuous manufacturing process, energy efficiency can be improved by: i) minimizing and balancing material use in product design; ii) reducing pressure loss in the extruder with thicker thicknesses (up to 20 % improvement); iii) optimizing product quality tolerances (up to 5 % improvement); iv) operating at high line velocities. Energy flexibility can be enhanced by: i) reducing profile thicknesses in product design; ii) adjusting line velocity based on utility prices; iii) scheduling sealing profiles according to utility cost ratios.

Therefore, the developed physics-informed digitalization strategy

Profile	Speed (m/min)	Total Elec (kWh/km)	Extruders	IR	MW	Conv	Auxiliar	Total Gas (m^3/hkm)
Line 1								
179	16.10 (12.88 – 19.32)	**96.29**	49.62	17.91	10.15	7.18	11.44	**22.99**
Line 2								
695	16.01 (12.81 – 19.21)	**182.19**	93.87	33.85	19.19	13.70	21.58	**24.01**
Line 3								
685	15.98 (12.78 – 19.18)	**115.09**	59.28	21.39	12.12	8.68	13.62	**23.97**
Line 4								
610	17.96 (14.37 – 21.55)	**109.97**	56.98	20.73	11.45	6.98	13.83	**22.79**
Line 5								
606	17.00 (13.60 – 20.40)	**108.85**	56.17	20.44	11.50	7.47	13.27	**17.09**
Line 6								
149	18.00 (14.40 – 21.60)	**55.84**	28.94	10.53	5.81	3.53	7.03	**16.99**

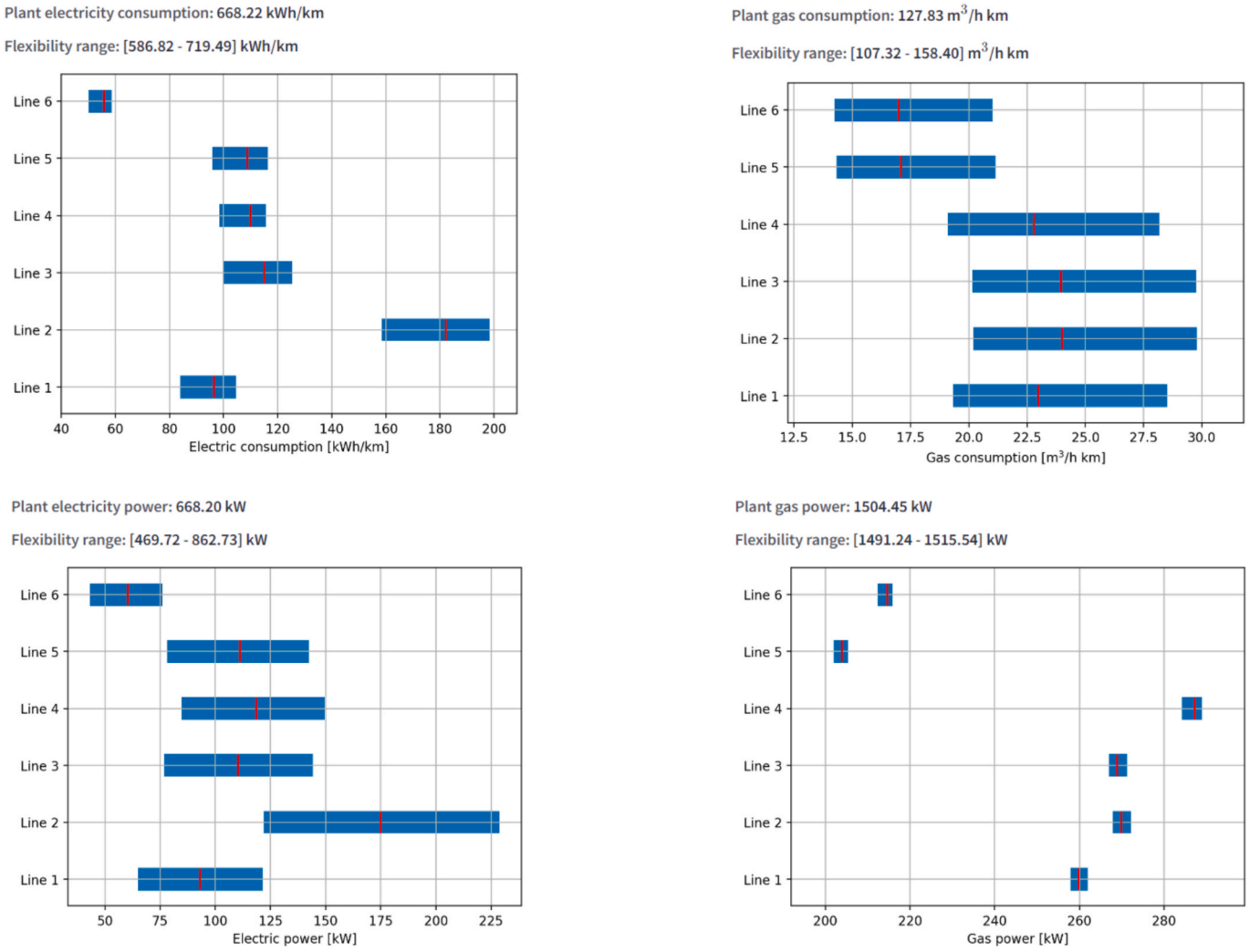

Fig. 16. Example of digitalization strategy deployment at an industrial manufacturing plant.

proposes different options to provide flexibility from different perspectives, so it can be used as a decision support tool for production planning and energy efficiency assessment in continuous manufacturing processes.

CRediT authorship contribution statement

María Herrando: Writing – original draft, Validation, Project administration, Investigation, Funding acquisition, Formal analysis, Conceptualization. **Ismael Viejo:** Writing – original draft, Visualization, Validation, Software, Methodology, Investigation, Formal analysis, Data curation, Conceptualization. **Susana Calvo:** Writing – review & editing,

Supervision, Resources, Funding acquisition. **Leticia A. Gracia:** Writing – review & editing, Supervision, Resources, Funding acquisition. **Salvador Izquierdo:** Writing – review & editing, Visualization, Supervision, Methodology, Funding acquisition, Conceptualization.

Declaration of competing interest

The authors declare the following financial interests/personal relationships which may be considered as potential competing interests: Ismael Viejo reports financial support was provided by European Commission. Maria Herrando reports financial support was provided by Spain Ministry of Science and Innovation. If there are other authors, they declare that they have no known competing financial interests or personal relationships that could have appeared to influence the work reported in this paper.

Acknowledgements

The authors would like to thank the company Standard Profil for providing information to model and validate the co-extrusion process modelling. This work was undertaken within the framework of the Juan de la Cierva Incorporación Fellowship awarded to Dr. María Herrando, funded by the Ministry of Science, Innovation and Universities (AEI) and co-founded by the EU, through the NextGeneration funds [grant number IJC2020-043717-I], as well as within the Flex4Fact project, funded by the European Commission under the Horizon Europe programme [HORIZON-CL4-2021-TWIN-TRANSITION-01-2, grant number 101058657].

Data availability

The authors do not have permission to share data.

References

[1] European commission. Delivering the European Green Deal - European Commission n.d. https://commission.europa.eu/strategy-and-policy/priorities-2019-2024/european-green-deal/delivering-european-green-deal_en (accessed October 22, 2024).
[2] U.S. Energy Information Administration. International Energy Outlook 2016 With Projections to 2040. 2016.
[3] Wan PK, Ranaboldo M, Burgio A, Caccamo C, Fragapane G. A Framework for Enabling Manufacturing Flexibility and Optimizing Industrial Demand Response Services. In: Alfnes E, Romsdal A, Strandhagen JO, von Cieminski G, Romero D, editors. APMS 2023. IFIP Advances in Information and Communication Technology, vol. 692, Cham: Springer Nature Switzerland; 2023. Doi: 10.1007/978-3-031-43688-8.
[4] Roth S, Thimmel M, Fischer J, Schopf M, Unterberger E, Braunreuther S, et al. Simulation-based analysis of energy flexible factories in a regional energy supply system. Procedia Manuf, vol. 33, Elsevier B.V.; 2019, p. 75–82. Doi: 10.1016/j.promfg.2019.04.011.
[5] Mourtzis D, Papakostas N, Mavrikios D, Makris S, Alexopoulos K. The role of simulation in digital manufacturing: Applications and outlook. Int J Comput Integr Manuf, vol. 28, Taylor and Francis Ltd.; 2015, p. 3–24. Doi: 10.1080/0951192X.2013.800234.
[6] Roth S, Schott P, Ebinger K, Halbrügge S, Kleinertz B, Köberlein J, et al. The challenges and opportunities of energy-flexible factories: a holistic case study of the model region augsburg in Germany. Sustainability (switzerland) 2020;12. https://doi.org/10.3390/su12010360.
[7] Fleschutz M, Bohlayer M, Braun M, Murphy MD. From prosumer to flexumer: Case study on the value of flexibility in decarbonizing the multi-energy system of a manufacturing company. Appl Energy 2023;347. https://doi.org/10.1016/j.apenergy.2023.121430.
[8] Mahmood M, Chowdhury P, Yeassin R, Hasan M, Ahmad T, Chowdhury NUR. Impacts of digitalization on smart grids, renewable energy, and demand response: an updated review of current applications. Energy Convers Manage: X 2024;24. https://doi.org/10.1016/j.ecmx.2024.100790.
[9] Benedetti M, Cesarotti V, Introna V. From energy targets setting to energy-aware operations control and back: an advanced methodology for energy efficient manufacturing. J Clean Prod 2017;167:1518–33. https://doi.org/10.1016/j.jclepro.2016.09.213.
[10] Herrando M, Viejo I, Teruel R, Izquierdo S. Development of Digital Twins to Optimise the Industrial Process Parameters in the Rubber Industry considering the Energy Vector as a Key Input Data. Proceedings of the 17th Conference on Sustainable Development of Energy, Water and Environment Systems, SDEWES Centre, 2022.
[11] Sproedt A, Plehn J, Schönsleben P, Herrmann C. A simulation-based decision support for eco-efficiency improvements in production systems. J Clean Prod 2015;105:389–405. https://doi.org/10.1016/j.jclepro.2014.12.082.
[12] Bleicher F, Duer F, Leobner I, Kovacic I, Heinzl B, Kastner W. Co-simulation environment for optimizing energy efficiency in production systems. CIRP Ann Manuf Technol 2014;63:441–4. https://doi.org/10.1016/j.cirp.2014.03.122.
[13] Dehning P, Thiede S, Mennenga M, Herrmann C. Factors influencing the energy intensity of automotive manufacturing plants. J Clean Prod 2017;142:2305–14. https://doi.org/10.1016/j.jclepro.2016.11.046.
[14] Rüßmann M, Lorenz M, Gerbert P, Waldner M, Justus J, Engel P, et al. Industry 4.0 The Future of Productivity and Growth in Manufacturing Industries. 2015.
[15] Thiele G, Heimann O, Grabowski K, Kruger J. Framework for energy efficiency optimization of industrial systems based on the control layer model. Procedia Manuf, vol. 33, Elsevier B.V.; 2019, p. 414–21. Doi: 10.1016/j.promfg.2019.04.051.
[16] Mawson VJ, Hughes BR. The development of modelling tools to improve energy efficiency in manufacturing processes and systems. J Manuf Syst 2019;51:95–105. https://doi.org/10.1016/j.jmsy.2019.04.008.
[17] Wright AJ, Oates MR, Greenough R. Concepts for dynamic modelling of energy-related flows in manufacturing. Appl Energy 2013;112:1342–8. https://doi.org/10.1016/j.apenergy.2013.01.056.
[18] Beier J, Thiede S, Herrmann C. Energy flexibility of manufacturing systems for variable renewable energy supply integration: real-time control method and simulation. J Clean Prod 2017;141:648–61. https://doi.org/10.1016/j.jclepro.2016.09.040.
[19] Lu Y, Peng T, Xu X. Energy-efficient cyber-physical production network: architecture and technologies. Comput Ind Eng 2019;129:56–66. https://doi.org/10.1016/j.cie.2019.01.025.
[20] Thongchul N, Kokossis A, Assabumrungrat S. A-Z of Biorefinery: A Comprehensive View. A-Z of Biorefinery, Elsevier; 2022, p. 1–759. Doi: 10.1016/B978-0-12-819248-1.00012-9.
[21] Hu C. Reactor design and selection for effective continuous manufacturing of pharmaceuticals. J Flow Chem 2021;11:243–63. https://doi.org/10.1007/s41981-021-00164-3.
[22] González-Ramírez JE, Leducq D, Arellano M, Alvarez G. Energy consumption optimization of a continuous ice cream process. Energy Convers Manag 2013;70:230–8. https://doi.org/10.1016/J.ENCONMAN.2013.03.015.
[23] Bajpai P. Raw Material and Pulp Making. Biermann's Handbook of Pulp and Paper, vol. 1. Third Edition, Elsevier; 2018, p. 1–647. Doi: 10.1016/B978-0-12-814240-0.05002-3.
[24] May G, Stahl B, Taisch M, Kiritsis D. Energy management in manufacturing: from literature review to a conceptual framework. J Clean Prod 2017;167:1464–89. https://doi.org/10.1016/J.JCLEPRO.2016.10.191.
[25] Das O, Zafar MH, Sanfilippo F, Rudra S, Kolhe ML. Advancements in digital twin technology and machine learning for energy systems: a comprehensive review of applications in smart grids, renewable energy, and electric vehicle optimisation. Energy Convers Manage: X 2024;24. https://doi.org/10.1016/j.ecmx.2024.100715.
[26] Nannapaneni S, Mahadevan S. Uncertainty quantification in performance evaluation of manufacturing processes. Proceedings of the IEEE International Conference on Big Data. 2014. https://doi.org/10.1109/BigData.2014.7004333.
[27] Kseib NS, Iaccarino G, Alonso JJ, Ihme M. Engineering SUD of M. Data Driven and Uncertainty Aware Physical Modeling. 2016.
[28] Oneto L, Orlandi I, Anguita D. Performance assessment and uncertainty quantification of predictive models for smart manufacturing systems. Proceedings of the IEEE International Conference on Big Data, Santa Clara, CA, USA: IEEE; 2015, p. 2959.
[29] Herrando M, Viejo I, Calvo S, Izquierdo S. Development of Digital Twins to increase Energy Flexibility and Energy Efficiency of Manufacturing Processes in the Rubber Industry. In: The 19th Conference on Sustainable Development of Energy, Water and Environment Systems (SDEWES); 2024. p. 042901–13.
[30] Stavropoulos P, Papacharalampopoulos A, Petridis D. A vision-based system for real-time defect detection: A rubber compound part case study. Procedia CIRP, vol. 93, Elsevier B.V.; 2020, p. 1230–5. Doi: 10.1016/j.procir.2020.04.159.
[31] Papacharalampopoulos A, Petridis D, Stavropoulos P. Experimental investigation of rubber extrusion process through vibrational testing. Procedia CIRP, vol. 93, Elsevier B.V.; 2020, p. 1236–40. Doi: 10.1016/j.procir.2020.04.160.
[32] Aschemann A, Hagen PF, Albers S, Rofallski R, Schwabe S, Dagher M, et al. Smart rubber extrusion line combining multiple sensor techniques for AI-based process control. Adv Eng Mater 2024. https://doi.org/10.1002/adem.202401316.
[33] Viejo I, Izquierdo S, Conde I, Zambrano V, Alcalá N, Gracia LA. A practical approach for uncertainty management in rubber manufacturing processes using physics-informed real-time models. Polymers (basel) 2022;14. https://doi.org/10.3390/polym14102049.
[34] Ha YS, Cho JR, Kim TH, Kim JH. Finite element analysis of rubber extrusion forming process for automobile weather strip. J Mater Process Technol 2008;201:168–73. https://doi.org/10.1016/j.jmatprotec.2007.11.290.
[35] del Coz Díaz JJ, García Nieto PJ, Ordieres Meré J, Bello GA. Computer simulation of the laminar nozzle flow of a non-Newtonian fluid in a rubber extrusion process by the finite volume method and experimental comparison. J Non Cryst Solids 2007;353:981–3. https://doi.org/10.1016/j.jnoncrysol.2006.12.067.
[36] Díaz JJ, Del C, Nieto PJG, García AB, Muñoz JG, Meré JO. Finite volume modeling of the non-isothermal flow of a non-Newtonian fluid in a rubber's extrusion die.

J Non Cryst Solids 2008;354:5334–6. https://doi.org/10.1016/j.jnoncrysol.2008.04.058.
[37] Alcalá N, Castrillón M, Izquierdo S, Gracia LA. Rubber material-model characterization for coupled thermo-mechanical vulcanization foaming processes. Polymers (basel) 2022. https://doi.org/10.3390/polym14061101.
[38] Le Bideau P, Ploteau JP, Dutournié P, Glouannec P. Experimental and modelling study of superficial elastomer vulcanization by short wave infrared radiation. Int J Therm Sci 2009;48:573–82. https://doi.org/10.1016/j.ijthermalsci.2008.03.016.
[39] Zakaria Z, Ariff ZM, Stephen SC. Effect of Foaming Temperature on Morphology and Compressive Properties of Ethylene propylene diena monomer rubber (EPDM). Foam 2007.
[40] Ariff ZM, Zakaria Z, Tay LH, Lee SY. Effect of foaming temperature and rubber grades on properties of natural rubber foams. J Appl Polym Sci 2008;107:2531–8. https://doi.org/10.1002/app.27375.
[41] Ghoreishy MHR. A state-of-the-art review on the mathematical modeling and computer simulation of rubber vulcanization process. Iran. Polym. J. (Engl. Ed.) 2016;25:89–109. https://doi.org/10.1007/s13726-015-0405-5.
[42] Shaft MA, Joshi K, Flumerfelt RW. Bubble size distributions in freely expanded polymer foams. vol. 52. 1997.
[43] Aloku GO, Yuan XF. Numerical simulation of polymer foaming process in extrusion flow. Chem Eng Sci 2010;65:3749–61. https://doi.org/10.1016/j.ces.2010.03.022.
[44] Restrepo-Zapata NC, Osswald TA, Hernández-Ortiz JP. Vulcanization of EPDM rubber compounds with and without blowing agents: Identification of reaction events and TTT-diagram using DSC data. Polym Eng Sci 2015;55:2073–88. https://doi.org/10.1002/pen.24049.
[45] Dassault Systems. Abaqus v2017 - General Purpose FE software, 2017.
[46] Ghoreishy MHR, Rafei M, Naderi G. Optimization of the vulcanization process of a thick rubber article using an advanced computer simulation technique. Rubber Chem Technol 2012;85:576–89. https://doi.org/10.5254/rct.12.88917.
[47] Zhang J, Tang W. Rubber curing process simulation based on parabola model. J. Wuhan Univers. Technol., Mater. Sci. Ed. 2013;28:150–6. https://doi.org/10.1007/s11595-013-0657-x.
[48] Wang Y, Su B, Wu J. Simulation and optimization of giant radial tire vulcanization process. Procedia Eng 2012;31:723–6. https://doi.org/10.1016/j.proeng.2012.01.1092.
[49] Vieira M, Pinto-Varela T, Barbosa-Póvoa AP. A model-based decision support framework for the optimisation of production planning in the biopharmaceutical industry. Comput Ind Eng 2019;129:354–67. https://doi.org/10.1016/j.cie.2019.01.045.
[50] Standard Profil. Standard Profil n.d. https://www.standardprofil.com/es (accessed October 22, 2024).
[51] Zambrano V, Rodríguez-Barrachina R, Calvo S, Izquierdo S. TWINKLE: A digital-twin-building kernel for real-time computer-aided engineering. SoftwareX 2020;11. Doi: 10.1016/j.softx.2020.100419.
[52] González D, Badías A, Alfaro I, Chinesta F, Cueto E. Model order reduction for real-time data assimilation through Extended Kalman Filters. Comput Methods Appl Mech Eng 2017;326:679–93. https://doi.org/10.1016/j.cma.2017.08.041.
[53] Marschik C, Roland W, Osswald TA. Melt conveying in single-screw extruders: modeling and simulation. Polymers (basel) 2022;14. https://doi.org/10.3390/polym14050875.